Gossamer Membrane Telescope

Thomas D. Ditto[1]
DeWitt Brothers Tool Company, Inc., New York, NY 10012

and

Jeffrey F. Friedman [2]
Universidad de Puerto Rico, Mayaguez, Puerto Rico, 00681

Diffraction grating microstructures covering a flat surface are effective in concentrating flux, but their angles of wavefront reconstruction at a secondary receiver are wavelength-dependent. By designing a secondary that exploits this wavelength dependency, we have invented an entirely new class of telescope, called a Dittoscope, which can acquire millions of high resolution spectra in an observation cycle. A diffraction grating primary objective is well suited for realization on a gossamer membrane substrate, since the effective optics are structures of wavelength proportions. Rigid framing structures that hold the membrane can take advantage of the tendency of the interior tensile membranes to generate flats. The gossamer membrane substrate need only provide sufficient tensile strength to withstand stretching forces and have flatness tolerances that correspond to the spectral resolution.

Nomenclature

POG	=	primary objective grating
λ	=	wave length of radiation
i	=	incident angle
r	=	receiving angle
p	=	grating period
n	=	diffraction order
$\Delta\lambda$	=	spectral resolution

I. Introduction

THIS disclosure reverses 400 years of telescope design. We show there is an alternative architecture for primary objectives that overcomes endemic observational limitations in reflector and refractor primary astronomical instruments while simultaneously conditioning a telescope for space deployment as a gossamer membrane.

The breadth of the innovation is potentially sweeping, but the present paper is merely the key to a door behind which can be found the disclosed option. The authors do not have a mature embodiment to report. This paper will show the embryonic form of a coherent instrument and outline pathways to its construction. This audience of readers has been chosen for its expertise in engineering gossamer structures. In other words, the authors come forward not to instruct so much as to seek a helping hand. Some readers who also specialize in telescope design may offer critical appraisals which invalidate the basic concept, and we welcome that dialogue, but short of such disqualification, the goal here is to initiate creative work in the development of a physical embodiment. A justification is laid out historically. Basic optical principles with critical features are parameterized. Empirical results are reported that corroborate the basic model. A roadmap for subsequent embodiments is suggested.

II. Background

A telescope primary objective collects incident radiation. Its size determines both amplification of flux and the angular resolution that resolves target features.

[1] VP, Research, 3d@taconic.net, AIAA Member.
[2] Professor, Departmento de Fisica, jeff@prtc.net

A. Historical development

Prior to the seventeenth century, all astronomical observations were premised on unaided human vision. Transits, sextants and astrolabes were invented to tabulate numerical data, but much of the sky was invisible, because objects were both too small and too faint.

1) Lens

Galileo did not invent the lens-based telescope, which traces to Dutch opticians, but he quickly realized that their placement of a secondary lens behind a primary objective would allow observations of the night sky. Galileo is credited with modifying the secondary objective with a negative lens so that the image was perceived as upright. The resulting tube-shaped instrument went largely unchanged for centuries. What Galileo did not understand was that the chromatic dispersion of a refraction magnifier would interfere with detailed observations. As lens primary objectives grew in size, chromatic aberration became intractable. Engineers chose longer and longer focal lengths to minimize the defect resulting in clumsy tracking mechanisms to keep synchronized with the transit of the stars.

2) Mirror

Newton did not invent the mirror-based telescope which was better described by Mersenne in 1636, but Newton understood that the mirror overcame the chromatic aberration of lenses. Newton's innovation was a plane secondary mirror which redirected the light to observer. Prior to Newton's 1670 folding mirror, attempts at reflection secondaries were beyond the mechanical skill of opticians of his day. Newton's primary objective mirror was spherical, leaving the parabolic reflector to be realized fifty years later. Eventually the mirror primary dominated over the lens. Its primary objective was free of chromatic aberration and the ray path could be folded to shrink the tube. Refractive elements that corrected subtle errors in the folding design were sometimes placed in front of the primary, but these were refractors were so thin as to be practically achromatic.

3) Diffraction Grating

The diffraction grating was not reported until 1785, over a century after Newton's telescope. The utility of the optic was later characterized in 1820 by Fraunhofer who used it as a disperser in the secondary to resolve absorption spectral lines. The discovery that stars produced the same spectral lines as the sun revolutionized astronomical observation, because the point source image of a star contained a new dimension in the parameter of its color. Diffraction gratings were the antithesis of mirrors, since they are characterized by their capacity to disperse, but, until recently, gratings were not thought to form images. The invention of holography in 1948 with its later physical embodiments in the 1960's removed that presumed limitation. Although still characterized by extreme chromatic aberration, at a fixed wavelength a hologram is every bit as capable of forming an image as a lens or a mirror.

B. Contemporary barriers in telescope performance

Angular resolution and flux collection are directly proportional to the size of the primary collector. The dominance of mirror collectors over the past century has led to four quantum leaps in mirror size. The 1.5 meter scale in the early twentieth century followed within a decade by the 2.5 meter scale. It took two decades before a 5 meter scale blank created by Corning led to the famous Palomar telescope which opened in 1948 and remained the largest in the world for over 40 years. Its mirror blank took 10 years to polish. In the 1980's, a series of projects pushed the scale of the mirror to 10 m, and examples of this scale are found world wide today.

Notably, no matter what the scale of the mirror, the secondary spectrometers of mirror primary telescopes were not capable of taking spectrograms in the same numbers as images of stars. Yet spectroscopy data is central to analysis of astronomical objects. For every 1,000 objects seen, there might be a few spectrograms of a single object.

Moreover, these twentieth century instruments were not suitable for space deployment, because the mirrors weigh many tons and have outside diameters far greater than payload bays and rocket fairings. Yet the benefit of space deployment has long been well understood. There are practical limits to ground-based observatories. First, the earth's atmosphere can be said to cancel out the benefit in resolving power provided by the larger mirrors. The atmosphere also filters out many of the electromagnetic wavelengths other than visible light. Secondly, the earth's rotation must be countered by elaborate gimbaled mounts that swing the huge telescope as it integrates over time. This leads to oddly complex shelters that open their roofs and pivot on their bases. Such mounts and buildings are so expensive, that as mirrors scale up, their infrastructure starts to cost more than the primary objective mirror being housed. None of these limitations apply under the space deployment paradigm.

C. Tensile mirrors

The search for stowable primary objectives with low aerial mass has been a preoccupation of NASA and other space agencies for decades. The appeal of a gossamer membrane is that its functionality in reflecting light is not affected by its thickness. The active mirror surface is measurable in microns, the native scale of membranes. However, insurmountable problems emerge when a parabolic reflector of astronomical telescope quality is figured

in thin plastic. Primary objective mirrors are necessarily three dimensional parabolic dishes or spherical mirrors with compensating secondaries. Formation of a dish in a tensile membrane has proven problematic.

An intuitive approach of an inflatable led to large collectors that held a figure suitable for long wavelengths, e.g., microwaves, but the approach fails at the sub-micron waves of visible light telescopes.[1] There are two problems. First, the sub wavelength tolerances cannot be prefigured on the ground before deployment. Secondly, the mirror is under a transparent film on the opposite side of the inflatable. The transparent film is not invisible, and adds artifacts to the incoming wave that exceed the worst kinds of atmospheric disturbance on earth.

When inflatables failed to provide a quick path to gossamer membrane space telescopes, other ideas were entertained. A two step magnifier where the primary is cylindrical is being investigated.[2] This limits the tensile structure to a trough which has a figure that can be maintained on a two dimensional space frame of the type that can be deployed from a Shuttle cargo bay. The effective collection is asymmetrical, but when secondary spectroscopy is the goal, this asymmetry propagates the desired functionality.

However, the most obvious figure for a tensile membrane is a flat surface, and this was examined as a possible configuration for a faceted primary objective which would be corrected in the secondary. Flats of 100 m scale were contemplated.[3] Preliminary models showed no insurmountable restrictions to making the flats, but the underlying concept of focusing the light proved daunting.

The question raised by the prior art is whether light can be concentrated using tensile gossamer membranes configured as flats.

III. Primary Objective Gratings

The native substrate figure of the diffraction grating is a flat surface. As such, POGs represent an available choice for a gossamer membrane telescope. Despite this fact, the literature shows no inquires into their possible use.

A. Prior Art

Historically, POGs had no power to concentrate flux. Dating to the nineteenth century, the traditional purpose of a POG has been slitless spectroscopy. The technique allows for Multiple Object Spectroscopy (MOS), a key performance feature that has become increasingly sought after since the utility of spectroscopy in astronomical observation was recognized. This is because a typical secondary spectrometer can acquire only one object per observation cycle, whereas its mirror primary can image tens of thousands of discrete points of light. The discrepancy between the rate of acquisition of spectrograms and images frustrates that study of astronomical objects.

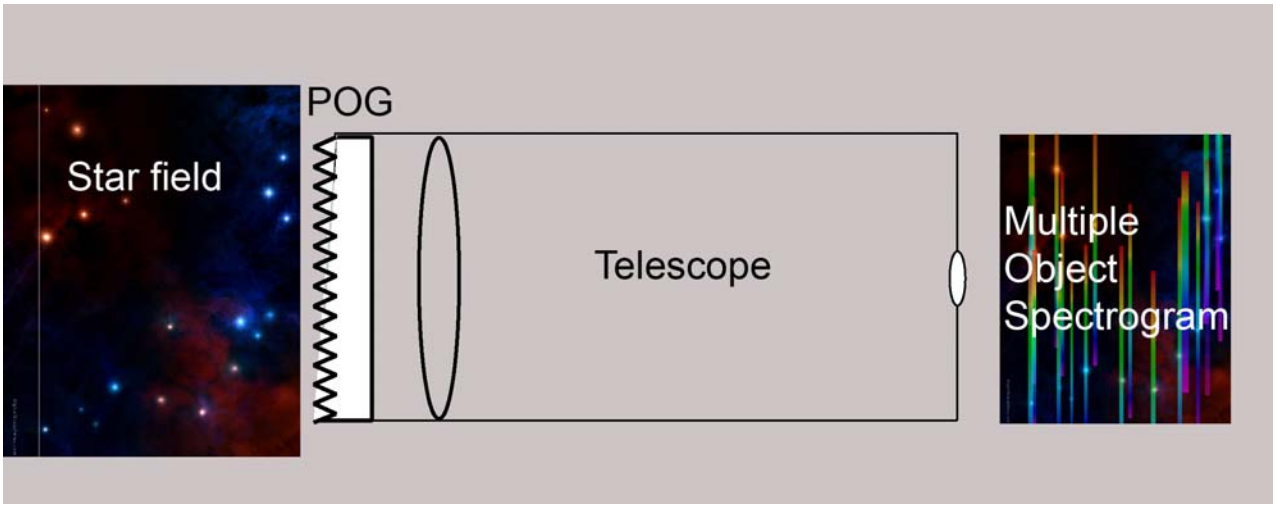

Figure 1. The Classical Primary Objective Grating Telescope. The plane grating does not concentrate the flux.

To achieve MOS implementations, a plane grating of low frequency is placed directly in front of an ordinary telescope. The spectrograms of all objects in the field of view can be recorded simultaneously at the image plane.

The diagrammatic representation of Fig. 1 illustrates the convention. Unfortunately, when stars are superimposed as spectra on the image plane, background radiation is superimposed on the spectra. Also, the spectra can easily overlap themselves, creating ambiguities. Finally, for spectra to fit within the image plane, the spectral signatures are short, as can be obtained with low frequency gratings. The resulting spectral resolution falls shy of many metrology standards practiced in the science.

B. The Innovation

An answer to the intrinsic problems posed by the conventional slitless objective grating spectrographs is found in an innovation similar to the invention that originally converted the magnifying lens into the telescope – a well conceived secondary. When a slit aperture spectrometer is used in the secondary of an objective grating telescope, the ambiguities of overlapping spectra are eliminated, because within the free spectral range the image in the secondary is restricted to a unique wavelength for each subtended angle incident upon the primary.

Resolving power and flux collection can be magnified by placing the secondary spectrometer at a grazing exodus configuration. If light striking the broad face of the POG is diffracted at angles approaching 90° off the grating plane normal, the secondary receiver size is a fraction of the size of the primary itself. When practiced with a plane grating, this magnification feature is anamorphic along the axis which is used to take the spectra.

These two innovations, a secondary spectrometer and collection at grazing exodus, lead to a new embodiment for an astronomical telescope, Fig 2.

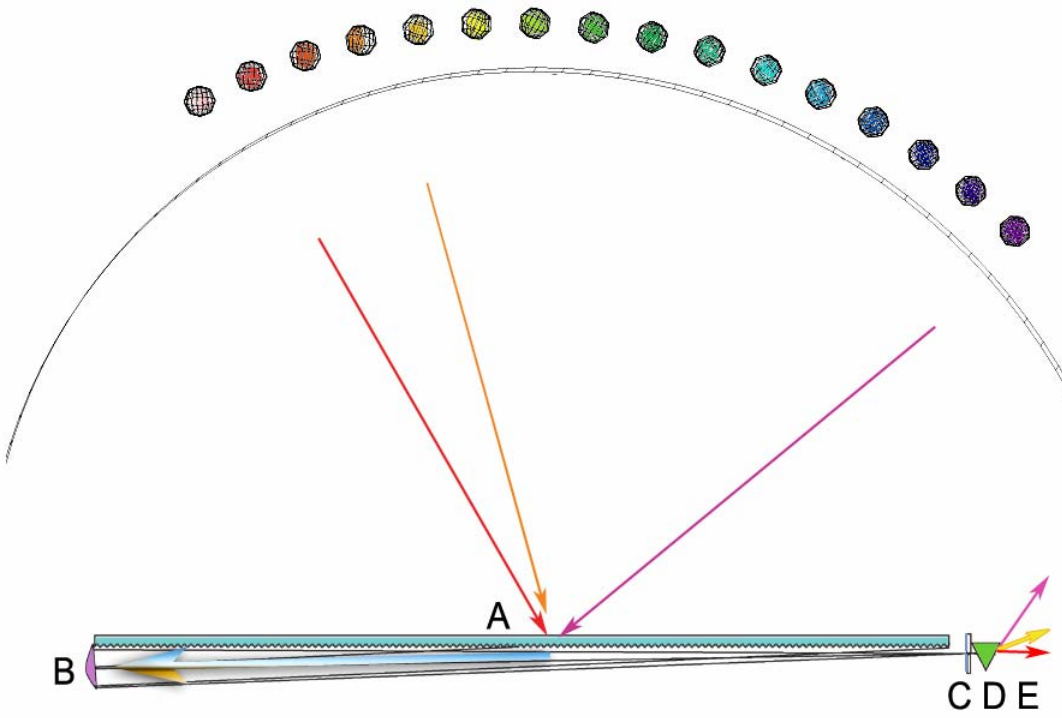

Figure 2. The Dittoscope. Light incident on POG A is diffracted to parabolic mirror B; focused on slit C before secondary dispersers D (shown as a prism). Wavelengths selected from correlated stars are then imaged at E.

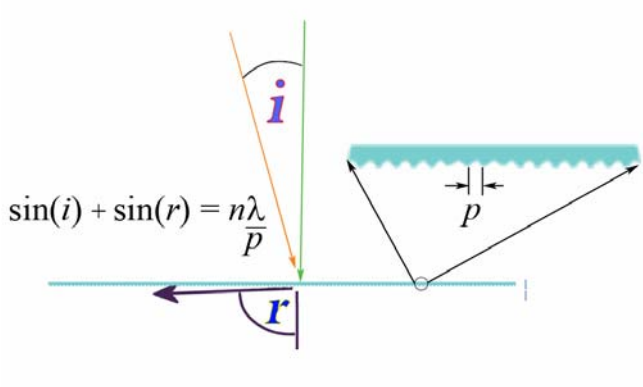

Figure 3. The Diffraction Equation

The geometric optics of diffraction are predicted by the diffraction equation, Fig 3. When the pitch of the grating p, the diffraction order n, and the receiving angle r are held constant, the angle of incidence i selects the received wavelength λ. The POG configured for grazing exodus is a special case. The conditions for establishing grazing exodus in the first-order require gratings with a pitch nearly the same as the wave lengths being dispersed. The grazing exodus case is $r \rightarrow 90°$. When r = 90°, it can be seen that if $p = \lambda$, then $i = 0$. When $p = \lambda$ the diffraction order is restricted to $n = \pm 1$.

One characteristic of these high frequency gratings where $\lambda \sim p$ is that they exhibit a broad free spectral range in the first-order. A wide free spectral range overcomes the coarse spectra typical of the low frequency gratings used in the original objective grating telescopes. We can quantify the behavior using the diffraction equation to calculate a typical case in the visible light regime, Figure 4. A central arc subtended around the zenith (where $i = 0$) of ±20° produces a 40° field-of-view with unambiguous spectra. Targets outside this window produce competing spectra in the same color bands that can be masked out with stops.

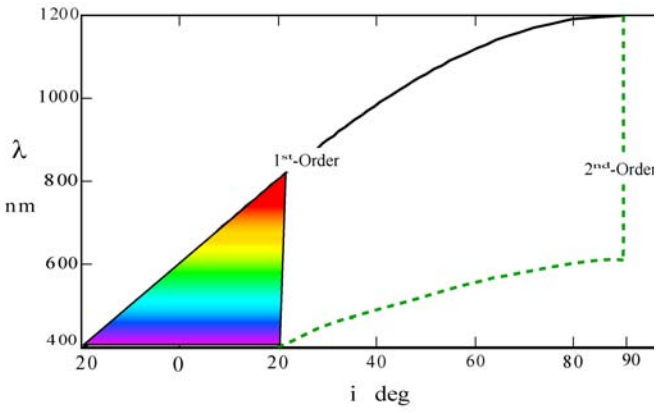

Figure 4. Free Spectral Range p = 600 nm at 87° grazing

In a reversal of an axiom going back to Newton that the best primary objective for an astronomical telescope exhibits the least chromatic aberration, it now can be said when spectrograms are the purpose of the instrument, the best primary objective is the one that achieves the greatest chromatic aberration. This is a type of grating with a short pitch that produces highly resolved discrete steps wave length $\Delta\lambda$ in the first-order.

Within the free spectral range, targets are recorded as a spectral spread where wavelength is correlated with incident angle i. A target's transit along the axis of diffraction provides a sequence of wave lengths over time that can be sequentially assembled into its spectrum.

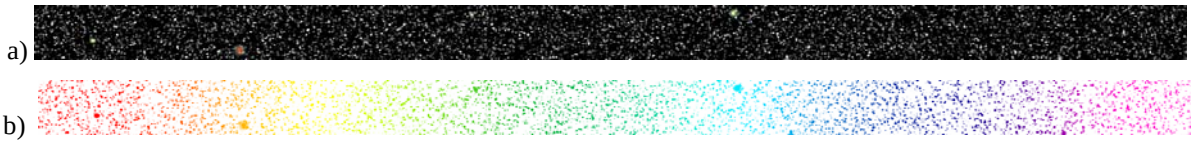

Figure 5.a) Firmament as seen by eye b) Instantaneous image at secondary spectrometer

On the focal plane of the secondary spectrometer, the full bandwidth image of the firmament (Fig. 5 a) is transformed into a spectral spread (Fig. 5 b). Although any one object is only seen at one wave length at one instant, the transit of all objects results in a temporal presentation of their full spectrum within the free spectral range. In terrestrial settings the process is implemented by exploiting the rotation of the planet. In space, the platform rotates. In both cases, the stars precess and parade their colors sequentially. Data reduction is a process of correlating the time with the angle of incidence.

C. Ribbon-shaped POG

This new design has interesting consequences for ground-based instruments which can enjoy apertures and collection areas orders of magnitude greater than any mirror and yet operate without any moving parts. However, for the purpose of the present discussion we consider how this configuration can be deployed in space.

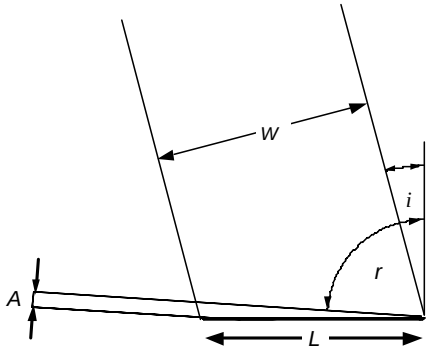

Figure 6, Magnification parameters

The anamorphic magnification that characterizes a grating at grazing exodus dictates that the primary collector has a ribbon-shaped aspect ratio where the longer dimension is along the axis of diffraction. The magnification M along the axis of diffraction is the ratio of the waist of the input beam W and the output aperture A (Fig. 6).

$$M = \frac{W}{A} \tag{1}$$

The magnification M and the length of the grating L are directly proportional to the receiving angle r while the waist W is inversely proportional to the incident angle i.

At the zenith where $i = 0°$ we can write:

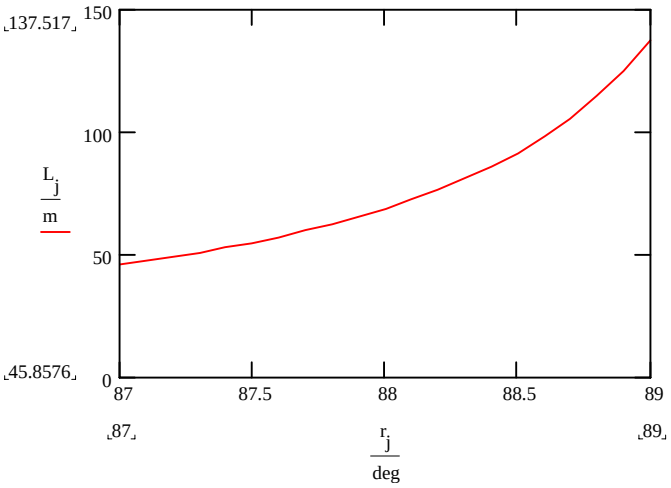

Figure 7 Length of POG using 2.5 m secondary mirror

$$A = L\frac{\sin(r)}{\tan(r)} \qquad (2)$$

which can be rewritten to correlate POG length to the selection of the diameter of the secondary mirror and its angle of grazing exodus.

$$L = \frac{A}{\sin(r)} \qquad (3)$$

In Fig. 7 we see the possible lengths of the POG when the secondary telescope has a mirror of 2.4 m, the type used in the Hubble Space Telescope. We calculate the lengths for grazing exodus angles between 87° and 89°. Lengths vary from 46 m to 138 m. Collection areas for these lengths would then vary from 111 m^2 to 330 m^2. These dimensions dwarf existing telescopes. For example, the Keck 10 m telescope has a working collection area of about 60 m^2.

When POGs are fabricated on gossamer membrane substrates, their considerable length can be transported on drum dispensers that fit within fairings and transporter payload bays. We can use the approximation for a grating length L in rolls by

$$L = \sum_{n=0}^{N} \pi(OD - nT) \qquad (4)$$

where OD is the outside diameter
T is membrane thickness
N is the number of wraps

$$N = \frac{OD - ID}{T} \qquad (5)$$

where ID is the inside diameter

Figure 8 illustrates sample calculations under this regime. The four traces show stowage on rolls of diameters of 10 cm, 50 cm, 1 m and 2.6 meters, with a packing thickness around the drum of 1 cm. Membrane thickness is carried out from 20 microns to over 1 mm. Clearly stowage of 100 m lengths is possible on almost any mandrill. When the drum is scaled to the size of the secondary telescope, kilometers of ribbon can be stowed. The choice of a drum for the roll stowage of the POG offers a cylindrical structural element that can be incorporated into the total telescope package, Fig. 9. The cylinder element could serve as the outside wall of the secondary telescope. The ribbon shape lends itself to the available storage dimensions in the transport vehicle, even though the transformed shape is a ribbon once deployed.

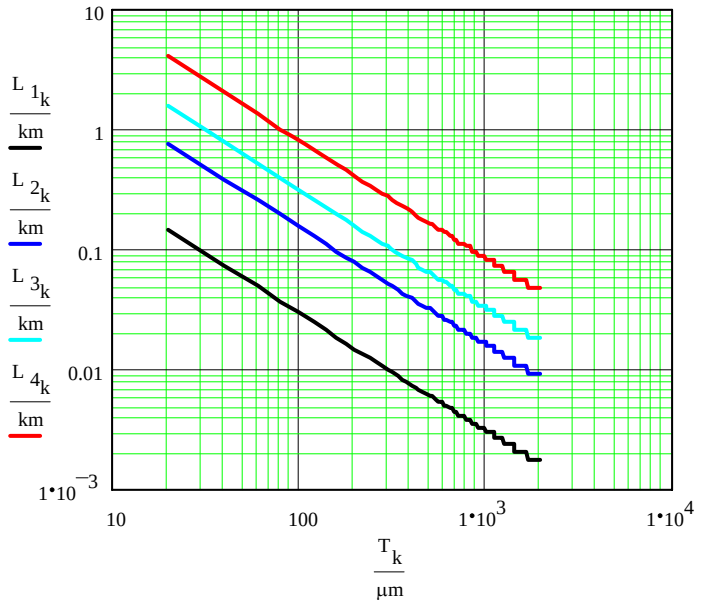

Figure 8, Stowable lengths of membrane of thicknesses up to 1 mm

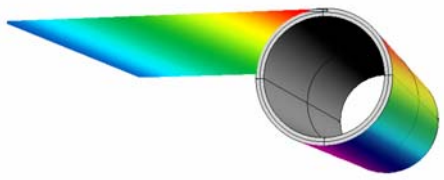

Figure 9, Roll stowage on a cylinder

D. Optical characteristics

A gossamer membrane optical element must maintain a figure within tolerances required by the telescope. Parabolic mirror gossamer membranes present structural challenges, because a three-dimensional surface must be figured in a tensile structure. Flats such as POGs reduce the structural problem to two dimensions, and the challenge is simply to eliminate the emergence of a third dimension. There is a limit to how flat a membrane can be stretched. The membrane itself will have variations in thickness, regardless of its overall structural flatness. We need to quantify the tolerances for flatness in order to establish the spectral resolution, $\Delta\lambda$.

The active magnification of a plane grating is along the axis perpendicular to the rulings. In a ribbon-shaped POG configured at grazing exodus, the grating rules run parallel to the short side. Because there is no magnification in this shorter dimension, the secondary parabolic mirror (Fig. 2, mirror B) establishes the angular resolution in one of the two dimensions. The analysis for performance is quite different in each direction.

1) Mirror

The POG must maintain a figure in its short dimension that will relay the incident wave to the secondary parabolic mirror near its diffraction limit. For example, the Sloan Digital Sky Survey (SDSS) 2.5 m mirror was polished to a tolerance of 100 nm end-to-end [4] and achieved a functional angular resolution on the order of 100 milliarcsec.[5] Plastic substrates have been developed with roughness tolerances of optical quality.[6] Given similar control over thickness, the challenge would then be to stretch the membrane to within 100 nm across 2.5 meters.

2) Grating

We assert that the tolerance for flatness in the diffraction dimension relaxes as the angle of grazing increases. This is because the diffraction image is formed by the constructive sum of in-phase waves originating from all grating grooves. When the light exits along the grating axis, variations in grating height have a negligible effect on the phase of the waves passing right over the grating surface and exiting to the side.

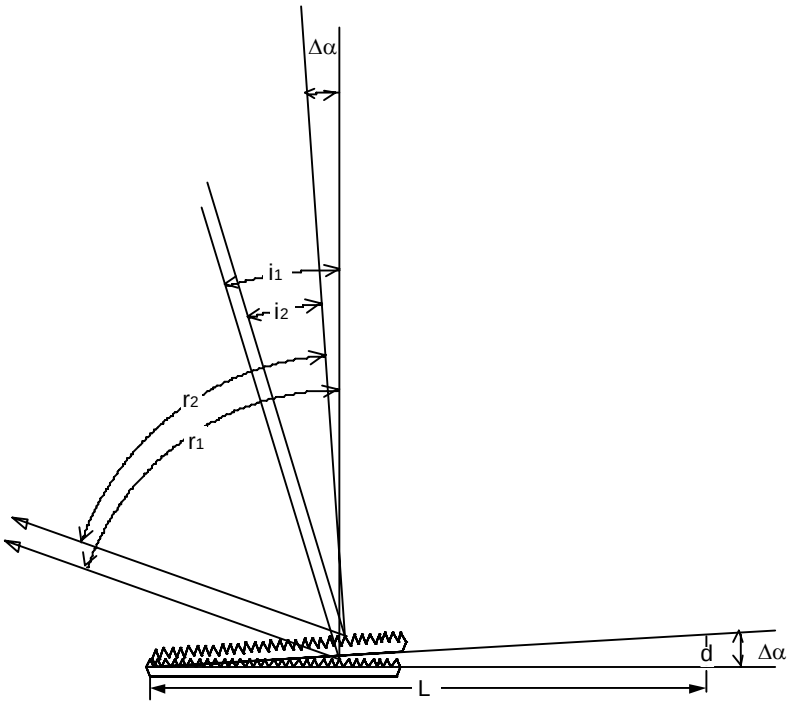

Figure 10 Parameterization of flatness tolerance specification

We can approximate the flatness tolerance for grazing exodus by using a displacement d over considerable length L. We compare two rays that are rotated by angle $\Delta\alpha$.

$$\Delta\alpha = \arctan\left[\frac{d}{L}\right] \qquad (6)$$

Angles of incidence i_1 and i_2 are rotated by $\Delta\alpha$ as are receiving angles r_1 and r_2.

Assuming we have determined incidence and receiving angles, we can compare the change in wavelength as a function of the surface flatness by calculating two wave lengths.

$$\Delta\lambda = \Delta\lambda_1 - \Delta\lambda_2 \qquad (7)$$

where λ is known from the diffraction equation.

$$\lambda = \frac{(\sin(i) + \sin(r))}{n} p \qquad (8)$$

This analysis suggests that when flatness is held to the same tolerance as the SDSS mirror, 100 nm over 2.5 m, the spectral resolution of the grating $\Delta\lambda$ in its worst case at the zenith is 0.000025 nm. We are examining incident radiation arriving near the zenith. When the light is at both grazing incidence and grazing exodus, there is no phase delay regardless of surface irregularity, and $\Delta\lambda \to 0$. Surface tolerance is well appreciated by diffraction grating manufacturers who often use float glass as a substrate where Ångstrom resolution is specified.

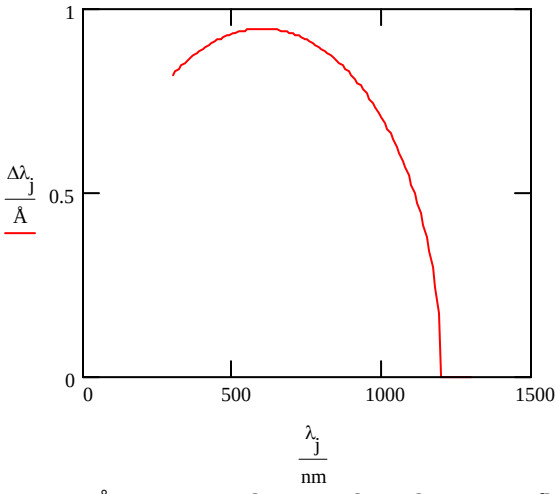

Figure 11 Ångstrom resolution with garden variety float glass rated at 8 waves per inch supporting a 600 nm grating configured at grazing exodus r = 88°

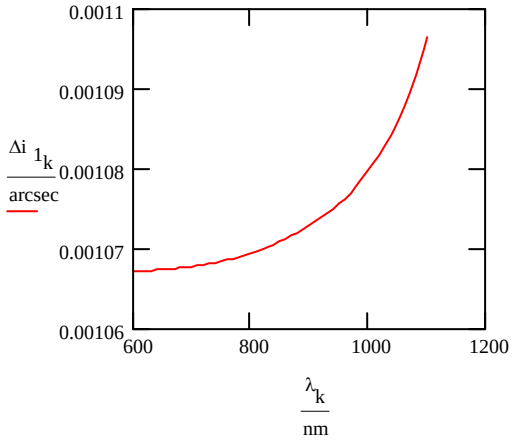

Figure 12 Resolved angles from 100 m POG with overall deviation in flatness restricted to ~ one wave

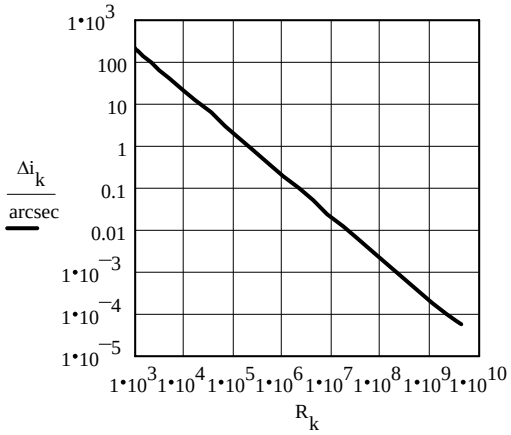

Figure 13 Δ*i* as a function of *R* using a log scale

We plot a relationship of λ vs. Δλ in Fig. 11 where the substrate is a modest quality float glass. In the example, grazing exodus angle $r = 88°$.

To correlate spectral resolution to angular resolution, we look at the linkage between the two. Small changes in wavelength correspond to small changes in the angle of incidence when the receiving angle r is fixed. We can determine Δi for the grating of Fig. 11 by taking the difference of the change in λ over one slope direction in the curve. We use:

$$\Delta i = \arcsin\left[\frac{\lambda}{p} - \sin(r)\right] - \arcsin\left[\frac{\lambda - \Delta\lambda}{p} - \arcsin(r)\right] \qquad (9)$$

We assume that $n = 1$ and exclude that term.

Using Eq. (9) we can graph another case for the grating of Figure 11 using a tighter tolerance for grating flatness of 600 nm over 100 m. This tolerance would be considered substandard for mirrors, and yet it certainly represents a challenge for large membrane structures. The error due to flatness is then shown to be on the order of 0.001 arcsec. This approximates the spacing of an exoplanet from its host star. The theoretical limit for Δi for a grating measured along the diffraction axis for a POG of 100 m length can also be calculated from the resolving power R on the basis of the grating length L:

$$R = \frac{L}{\lambda} \qquad (10)$$

Δλ can then be known from

$$\Delta\lambda = \frac{\lambda}{R} \qquad (11)$$

For 600 nm infrared radiation incident along a 100 m grating, $R = 1.667 * 10^8$. At this resolving power the limit of Δλ is $3.6 * 10^{-5}$ Å. With Eq. (9) we can determine a theoretical limit of Δi. For a 100 m POG, p = 600 nm, we calculate that Δi = 1.245 milliarcsec. We show the generalized relationship at this wavelength for a wider set of first-order resolving powers in Fig. 13. The upshot is that if the POG can be kept flat to a tolerance that falls within the wavelength of the light it is measuring, it can achieve a level of performance that is close to the theoretical limit of its resolving power.

These calculations further indicate that flatness tolerances for diffraction gratings are different than figure tolerances for mirrors. Designing a space borne POG presents asymmetrical tolerances for the width vs. its length with the shorter side requiring the higher level of precision.

E. Embodiments

Space deployment of a gossamer membrane POG ribbon bears a structural similarity to space tethers which have been studied for formation flying.[7] The tether concept has dynamic and stationary configurations. Replacing a tether cable with a ribbon introduces a planar twist parameter not yet characterized, but the stretching forces are similar.

a) The Bolo

The angle of incidence on the POG determines the wavelength at the secondary spectrometer, so it follows that the instrument should undergo a rotation. The rate of rotation can be selected to optimize the integration time for each wavelength. In LEO, the centrifugal forces are influenced by microgravity and gravity trapped particles, so the configuration lends itself better to stations at LaGrange points. The instrument can support up to four secondary telescopes which takes advantage of flux collected in inverse sequences of spectral spread, Fig. 14.

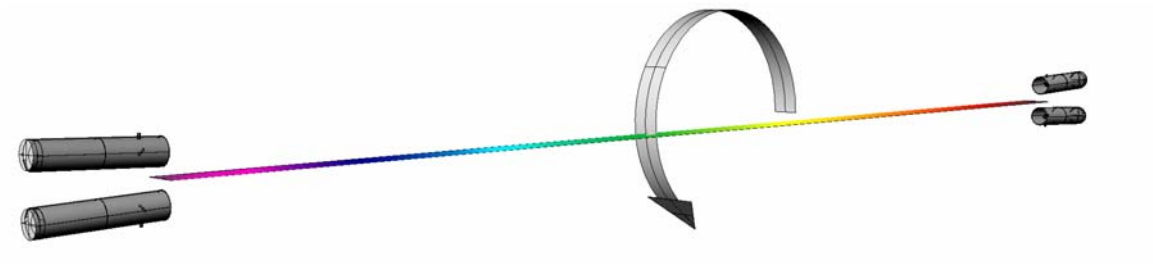

Figure 14, The Bolo. A symmetrical distribution of secondaries in a rotating platform

Inertial forces exerted when the instrument is placed in rotation provide useful force vectors to keep the spacecraft stable and the membrane stretched flat. The scanning motion is reminiscent of a radar sweep. The process could conceivably acquire all spectra from all targets in a band of ~1° x 360° over the course of a single rotational cycle. This might be as many as tens of millions of discrete spectra, depending on the density and intensity of the radiation sources in view.

b) Geostationary

Another option for deployment would be a configuration where the POG was inserted into geostationary orbit. A natural stationary posture of a ribbon in geostationary orbit is to point directly toward the center of the earth as the centrifugal force pulling the distal extremity is balanced by the gravitational force pulling the proximal side toward the earth. The integration time would then be locked into the diurnal period of the earth's rotation which we have shown elsewhere is 2.3 seconds/ Å.[8]

IV. Conclusion

We have introduced the concept of a gossamer membrane telescope based on a flat primary objective grating. The concept lends itself to space deployment. The secondary optics can be drawn from prior art in reflection telescope design, but the primary objective is completely novel. The primary objective is easily stowed and can easily be deployed from drum cylinders. Once deployed, the primary can enjoy a large collection area. Apertures capable of milliarcsecond resolution are possible. Tolerances along the longest axis are relaxed when compared with mirror primary objectives.

Acknowledgments

This research was supported by a Phase I Fellowship from the NASA Institute for Advanced Concepts, USRA Research Subaward No. 07605-003-060.

References

[1] Palisoc *et al*, "Geometry attained by pressurized membranes," *Space Telescopes and Instruments V*, SPIE Vol. 3356 (1998), pp. 747-757

[2] Mark W. Dragovan, "Precision formed membrane surface for electromagnetic radiation concentration and method of forming same," US Patent 6,502,944, Jan 7, 2003, Figs 1-5 and 16

[3] Sabatke and Burge, "Imaging Interferometers Using Flat Primary Segments," *Highly Innovative Space Telescope Concepts*, SPIE Vol. 4849 (2002), pp. 365-371

[4] Gunn *et al*, "The 2.5 m Telescope of the Sloan Digital Sky Survey," *The Astronomical Journal*, Vol. 131 (April 2006), pp. 2332 - 2359
[5] Pier *et al*, "Astrometric Calibration of the Sloan Digital Sky Survey," *The Astronomical Journal*, Vol. 125 (March 2003) pp. 1559-1579
[6] Patrick *et a*l, "Polymer material and casting process development for reduced manufacturing cost of spaceborne optics," *Optical Materials and Structures Technologies*, SPIE, Vol. 5179 (2003), pp. 127-132
[7] Farley and Quinn, "Tethered Formation Configurations: Meeting the Scientific Objectives of Large Aperture and Interferometric Science," *AIAA Space 2001*, AIAA Paper 2001-4770
[8] Thomas Ditto, "The Dittoscope," *Future Giant Telescopes*, SPIE, Vol. 4840 (2003), pp. 586-597